University of Glasgow

DEPARTMENT OF

AEROSPACE ENGINEERING

Validation of a Blade-Element Helicopter Model for Large-Amplitude Manoeuvres

S. S. Houston

Validation of a Blade-Element Helicopter Model for Large-Amplitude Manoeuvres

S. S. Houston

Dept. of Aerospace Engineering

University of Glasgow

Scotland

G12 8QQ

Departmental Report No. 9605

May 1996

Validation of a Blade-Element Helicopter Model for Large-Amplitude Manoeuvres

S. S. Houston
Dept. of Aerospace Engineering
University of Glasgow
Scotland
G12 8QQ

Abstract

The contemporary approach to helicopter mathematical modelling in simulation for handling qualities applications, is to represent each blade individually. This allows incorporation of effects not possible with a multiblade disc representation of the rotor system. This Paper addresses the validation of such a model, which is uniquely performed for large amplitude manoeuvres, using a recently-developed approach to inverse simulation. The method is reviewed in the context of model validation, and comparisons between simulation and actual data are presented for a Puma helicopter executing sidestep manoeuvres in low-speed flight. The focus for interpreting the results is in the area of wake modelling. It is concluded that further developments are necessary in this area if helicopter flight mechanics models are to be used in simulation of role-related flight.

Nomenclature

A	matrix of state vector acceleration coefficients
C_0	apparent mass factor
$[L]$	dynamic inflow static gain matrix
L	rolling moment (Nm)

$L_{\theta_{1c}}$	rolling moment derivative with respect to lateral cyclic (1/s)
M	pitching moment (Nm)
T	thrust, wind/hub transformation matrix (N or rad)
R	rotor radius (m)
r	radial position on rotor disc (m)
$v_{i_0}, v_{1_s}, v_{1_c}$	components of induced velocity (m/s)
$v_i(r, \psi)$	induced velocity at position (r, ψ) (m/s)
v_T	wake velocity (m/s)
v_m	wake mass flow velocity (m/s)
v_{i_m}	momentum induced velocity (m/s)
$u_{hub}, v_{hub}, w_{hub}$	non-rotating rotor hub velocities (m/s)
ρ	air density (kg/m^3)
$[\tau]$	time constant matrix (s)
χ	wake skew angle (rad)
Δ	transformation angle, wind/hub axes (rad)
$\underline{x}$	state vector
$\underline{u}$	control vector
$\underline{y}(t_k)$	output vector at time t_k
$\underline{u}(t_k)$	control vector at time t_k
$\underline{y}(t_{k+1})$	output vector at time t_{k+1}
$\underline{u}(t_{k+1})$	control vector at time t_{k+1}
t_k	time at kth point in flight data (s)
t_{k+1}	time at $(k+1)$th point in flight data (s)
ϕ, θ, ψ	roll, pitch and yaw angles (rad)

Subscripts

aero	aerodynamic
des	desired
wind	wind axes

Introduction

The mathematical modelling of helicopters for stability, control and handling qualities applications has assumed increased importance in design and analysis over the last 15 years. This is due to the need to remedy known deficiencies, and has been facilitated by the fact that computing power has allowed improved modelling to be accommodated in real-time as well as non real-time simulations. Padfield, Ref. 1, has defined and summarised the characteristics of three different levels of helicopter model. Moving from Level 1 to Level 2 sees the introduction of individual blade representations of the rotors, e.g. Refs. 2-5. This allows easy incorporation of aerodynamic and geometric non-linearity. Level 2 models are the state-of-the-art for stability, control and handling qualities applications. Currently, rotor wake models seek to calculate the induced velocity at a blade station and are of finite, 3-state form which is then transformed algebraically into induced velocity anywhere on a blade. Padfield proposes that Level 3 models will dispense with this approach and rely instead on the type of non-finite state free- or prescribed-wake theories to be found in aerodynamic performance codes used for detailed design.

The development of finite state induced velocity models for flight mechanics work is well summarised in Chen's review paper, Ref. 6, where the extensive literature attributed to Peters is rightly to the fore. The seminal work of Peters and many co-authors in this field has formed the basis of rotor wake modelling for simulation, e.g. Refs. 7, 8. The wake model used in this application is the Peters representation, and will be reviewed later as it forms a focus for this validation exercise.

Background

Arguably, validation methods have not kept pace with the development of the models themselves. Ref. 9 documents contemporary methods and results in model validation, which revolve around the derivation of small-perturbation, linearised

models from flight test data. Although Level 2 models can be reduced to this form, Ref. 10, they are physically capable of representing large amplitude manoeuvres as well. The value of simulation in this regime is that the model can be exercised in limiting or maximum performance manoeuvres. Intuitively, validation of the model in this area is its ultimate test. Bradley et al, Ref. 11, have proposed the use of inverse methods for this purpose, but it is only recently that an appropriate algorithm has been written specifically for a Level 2 model, Ref. 12.

Some recent studies have highlighted the need for validation across a wide range of amplitudes in manoeuvres. This is because validation has focused exclusively on small-amplitude inputs, and the results (in relation to mathematical modelling) warrant broadening the scope of investigation. For example, AGARD Working Group 18, Ref. 9, synthesised results from flight test data in linearised derivative or frequency response form. Application of this results database to initial validation of the model that is the focus for the study in this Paper was inconclusive, Ref. 10, due to the variability in the flight estimates of derivatives. Tischler's work, Ref. 13 for example, has emphasised the need for accurate models of higher order effects in the design of high bandwidth flight control systems. The recent work of Tournour and Celi, Ref. 14 is a good illustration of the validation of some of the issues and features unique to blade element models. However, here again the validation is based on small amplitude manoeuvres, specifically frequency sweep inputs, that were used to derive frequency responses. Nonetheless, some significant conclusions were produced in relation to the significance of blade elasticity and wake models.

Mathematical Model

The key features of the mathematical model used are summarised in Table 1. The model takes the form

$$A\dot{\underline{x}} = f(\underline{x},\underline{u})$$

where the state vector $\underline{x}$ contains the airframe translational and angular velocity, blade flap, lag and feather angles and rates for each blade on each rotor, the induced velocity states for each rotor wake as well as rotorspeed and engine torque. The control vector $\underline{u}$ contains the three main rotor and the single tail rotor control. In total, there are then 72 non-linear, periodic ordinary differential equations describing the coupled rotor/airframe behaviour of the Puma used for this study.

Table 1 Mathematical model description

Model item	Characteristics
Rotor dynamics (both rotors)	• up to 10 individually-modelled rigid blades • fully-coupled flap, lag and feather motion • blade attachment by offset hinges & springs • linear lag damper
Rotor loads	• aerodynamic and inertial loads represented by up to 10 elements per blade
Blade aerodynamics	• lookup tables for lift and drag as function of angle-of-attack and Mach number
Wake model	• Peters' dynamic inflow model • uniform and harmonic components of inflow • rudimentary interaction with tail surfaces • ground effect
Transmission	• coupled rotorspeed and engine dynamics • up to 3 engines • geared or independently-controlled rotor torque
Airframe	• fuselage, tailplane and fin aerodynamics by lookup tables or polynomial functions
Atmosphere	• International Standard Atmosphere • provision for variation of sea-level temperature and pressure

It is not feasible to describe fully the mathematical model development here. However, the original mathematical model definition used as the basis of the current implementation is described in Ref. 2, and the generation of rotor forces and moments in particular is described in Ref. 10. Since the dynamic inflow model will serve as a focus for the validation, it is appropriate to describe it here. The representation used is taken from Chen, Ref. 6, although the original model development is due to Peters, Refs. 7, 8.

The basic form of induced velocity at any azimuth and radial station over the rotor is given by

$$v_i(r,\psi) = v_{i_0} + \frac{r}{R} v_{1_s} \sin\psi + \frac{r}{R} v_{1_c} \cos\psi$$

The induced velocity $v_i(r,\psi)$ appears explicitly in the aerodynamic model to influence the blade element angle of attack. The three states v_{i_0}, v_{1_s} and v_{1_c} are calculated as follows.

The differential equations describing the induced velocity state behaviour for the rotor are given by

$$[\tau]\begin{bmatrix}\dot{v}_{i_0}\\ \dot{v}_{1_s}\\ \dot{v}_{1_c}\end{bmatrix}_{wind} = -\begin{bmatrix}v_{i_0}\\ v_{1_s}\\ v_{1_c}\end{bmatrix}_{wind} + [L]\begin{bmatrix}T_{aero}\\ L_{aero}\\ M_{aero}\end{bmatrix}_{wind}$$

where

$$[\tau]=\begin{bmatrix} \dfrac{4R}{3\pi v_T C_0} & 0 & \dfrac{-R\tan(\chi/2)}{12v_m} \\ 0 & \dfrac{64R}{45\pi v_m(1+\cos\chi)} & 0 \\ \dfrac{5R\tan(\chi/2)}{8v_T} & 0 & \dfrac{64R\cos\chi}{45\pi v_m(1+\cos\chi)} \end{bmatrix}$$

and

$$L=\frac{1}{\rho\pi R^3}\begin{bmatrix} \dfrac{R}{2v_T} & 0 & \dfrac{15\pi\tan(\chi/2)}{64v_m} \\ 0 & \dfrac{-4}{v_m(1+\cos\chi)} & 0 \\ \dfrac{15\pi\tan(\chi/2)}{64v_T} & 0 & \dfrac{-4\cos\chi}{v_m(1+\cos\chi)} \end{bmatrix}$$

The term C_0 in the time constant matrix takes the value 1 or 0.64, depending on whether or not the blades are twisted. These wind axes equations can be transformed into an appropriate set of non-rotating rotor hub axes by applying the transformation

$$T=\begin{bmatrix} 1 & 0 & 0 \\ 0 & \cos\Delta & \sin\Delta \\ 0 & -\sin\Delta & \cos\Delta \end{bmatrix}$$

where

$$\tan\Delta=\frac{v_{hub}}{u_{hub}}$$

The velocities v_T and v_m are given by

$$v_T=\sqrt{u_{hub}^2+v_{hub}^2+\left(v_{i_m}-w_{hub}\right)^2}$$

$$v_m = \frac{u_{hub}^2 + v_{hub}^2 + \left(v_{i_m} - w_{hub}\right)\left[2v_{i_m} - w_{hub}\right]}{v_T}$$

and the wake skew angle by

$$\tan\chi = \frac{\sqrt{u_{hub}^2 + v_{hub}^2}}{v_{i_m} - w_{hub}}$$

Inverse Simulation

Inverse methods in engineering problems are commonplace. In aircraft flight mechanics the terminology is used to describe a process whereby instead of specifying a control vector $\underline{u}$ and calculating the vehicle state, particular aspects of the state are specified, and the required control vector $\underline{u}$ is calculated. It is usual to specify the required state in terms of flight path variables or trajectory information. In principle, constraining the vehicle mathematical model in this way allows non real-time simulation of manoeuvres that is not possible using a forward approach because modelling inadequacies give rise to errors that are propagated and magnified over time with integration of the vehicle equations of motion.

The extensive literature due to Thomson, e.g. Refs. 11, 15, 16, documents development and application of inverse methods for helicopters. This has been for a Level 1 model, which can be recast explicitly in inverse form. However, the proliferation of states that occurs with Level 2 models, specifically in the blade degrees of freedom, render this approach impossible, as insufficient constraint information is available. The approach proposed by Rutherford and Thomson, Ref. 12, is based on a model-following optimisation scheme with a strong predictor/corrector element, which has been used previously by Gao and Hess, Ref. 17, amongst others. The equations of motion remain in standard form, and a time-

marching iterative search technique is used to find controls that satisfy the constraint requirement, as follows.

The discrete constraint vector $\underline{y}(t_k)$ is a non-linear function of the states and controls,

$$\underline{y}(t_k) = F(\underline{x}(t_k), \underline{u}(t_k))$$

If the controls $\underline{u}(t_k)$ are to be held constant over some application interval T and a zero-order hold employed, then the output at time t_{k+1} is some function of the control inputs at t_k , i.e.

$$\underline{y}(t_{k+1}) = G(\underline{u}(t_k))$$

The desired output vector, which the constraint vector variables are to follow, is obtained from the flight test data, enabling the definition of an error matrix

$$E(\underline{u}(t_k)) = \underline{y}(t_{k+1}) - \underline{y}_{des}(t_{k+1})$$

i.e.

$$E(\underline{u}(t_k)) = G(\underline{u}(t_k)) - \underline{y}_{des}(t_{k+1})$$

The control vector $\underline{u}(t_k)$ required to minimise $E(\underline{u}(t_k))$ is found using a Newton-Raphson method,

$$\underline{u}_{i+1}(t_k) = \underline{u}_i(t_k) - (J[G(\underline{u}(t_k)])^{-1} E(\underline{u}_i(t_k))$$

where $J[G(\underline{u}(t_k)]$ is the Jacobian matrix

$$J|_{i,j} = \left[\partial E_i(\underline{u}(t_k)) \Big/ \partial \underline{u}_j(t_k) \right]$$

which is evaluated numerically using a forwards/backwards difference scheme. The iteration loop is terminated when $E(\underline{u}(t_k))$ falls below pre-set tolerances. The control vector is then fed into the simulation and the process repeated for the next time interval.

In Rutherford and Thomson's original application of this method to the helicopter problem, the output vector elements consisted of trajectory information. This Paper proposes that the aircraft attitude and height error is a more appropriate formulation for the model validation problem, i.e.

$$\underline{y}(t_{k+1}) = \begin{bmatrix} \phi_{k+1} \\ \theta_{k+1} \\ \psi_{k+1} \\ h_{k+1} \end{bmatrix} \text{ and } \underline{y}_{des}(t_{k+1}) = \begin{bmatrix} \phi_{des} \\ \theta_{des} \\ \psi_{des} \\ h_{des} \end{bmatrix}$$

Results

Two manoeuvres are presented, a sidestep to the left, and one to the right. The flight test data were gathered using a Puma helicopter. Table 2 gives leading data for this aircraft. The manoeuvres start and end in a hover, and the nominal manoeuvre distance is 60 m. The aircraft exceeds 25 knots sideways during both manoeuvres. These are limiting manoeuvres in that a control limit (on main rotor collective pitch angle) is reached.

Influence of manoeuvre direction

Figures 1a and 1b show the roll, pitch and yaw attitudes for the manoeuvres to left and right, respectively. It is clear the application of the algorithm has been successful, as the helicopter's attitude is matched accurately by the model.

Table 2 Aircraft leading data

Rotor data		
Parameter	**Main rotor**	**Tail rotor**
Number of blades	4	5
Rotor radius	7.498 m	1.518 m
Blade mass	91 kg	2 kg
Distribution	non-uniform	non-uniform
Twist	6 deg at tip	0 deg
Chord	0.533 m	0.146 m
Airfoil section	NACA 0012	NACA 0012
Mach number range	0 - 0.8	0 - 0.8
Angle-of-attack range	±21 deg	±21 deg
Hinge offset	0.0387	0.0720
Number of elements	10	10
Direction of rotation	clockwise from above	clockwise from port
Shaft orientation	5 deg forward	90 deg to right
Nominal rotorspeed	28.5 r/s	137.8 r/s
Airframe data		
Aircraft mass	5805 kg	
I_{xx}	9638 kgm^2	
I_{yy}	33240 kgm^2	
I_{zz}	25889 kgm^2	
I_{xz}	2226 kgm^2	

Figures 2a and 2b show flight and model comparisons of the control time histories required to fly the manoeuvres to left and right, respectively. The inputs required to manoeuvre to the left are matched fairly well by the model. The model controls return to the correct trim, any mismatch being during the translating part of the manoeuvre. Main rotor collective is well-matched by the model, the tail rotor collective pitch less well so. The pulses in lateral cyclic required to initiate and stop the manoeuvre are underestimated by 50%. This is consistent with results from small-perturbation validation at 80 knots (no hover data are available). Using the linearisation method described in Ref. 10, the lateral cyclic pitch control derivative

$L_{\theta_{1c}}$ is calculated to be 51.04/s, whereas Ref. 9 indicates that the flight-derived value is 27/s. This would mean that approximately half the lateral cyclic pitch is required by the model to generate the same roll moment.

A similar assessment can be made of the comparisons during flight to the right. However, a further very significant difference exists. There is no symmetry between lateral cyclic pitch inputs required to fly to right and left. The model makes a reasonable attempt to replicate this, but is only able to do so up to about 8 s. The longitudinal cyclic pitch is poorly matched, and together these results indicate a significant event at about 5 s. At this time, the tail rotor model experiences the maximum axial velocity which is in a direction consistent with flight into the vortex ring region, Figure 3. The dynamic inflow model theory used, is inappropriate for these conditions. The time-wise extent of the positive axial velocity is consistent with the period of mismatch in controls between flight and model. Since the Puma's tail rotor is mounted high on the tail fin, substantial roll moments are produced. It is therefore reasonable to surmise that since the tail rotor model is operating in an inappropriate region, the rolling moments that it produces are inappropriate.

Numerically, axial flight of the rotor that gives rise to a positive value of w_{hub} (tending to move in a direction that in reality is towards the vortex ring condition) will tend to make v_m and v_T small. As a consequence the static gain and time constant matrices $[L]$ and $[\tau]$ will tend to increase in magnitude. The extent to which this occurs is significant, as evidenced by the tail rotor results for right sideways flight.

For example, Figure 4 shows v_{I_s} and v_{I_c} for the tail rotor model during flight to the left, where the tail rotor induced velocity model operates in an appropriate regime for the theory. A tail rotor blade flap angle time history is shown in Figure 5. Corresponding results for flight to the right are given in Figures 6 and 7. It is clear that the latter exceed physically-realistic values. Again, this occurs around the point

in time when the tail rotor experiences the largest adverse axial velocity. It can be argued then that the ability of the model to replicate at least some of the significant feature of the right sidestep (in terms of lateral cyclic), is compromised by resulting features that are physically unrealistic.

Rigid and non-rigid wake assumption

The harmonic elements of the gain and time constant matrices are increased by a factor of two if the wake is assumed to be "rigid" during the development of the theory, Ref. 6. Figure 8 shows that the cyclic pitch required to fly the left sidestep is insensitive to the wake assumption used, as the results are near-identical to those in Figure 2a. Indeed, if the harmonic components are set to zero in the calculation of the blade loads, there is also little change in the cyclic pitch relative to Figures 2a or 8. It could be argued in this latter case that the model cyclic pitch compares more favourably with flight than either the rigid, or non-rigid wake assumptions, certainly between 5 and 10 s.

It is somewhat disappointing that none of these three options does anything to improve the lateral cyclic pitch pulse comparisons. Induced velocity issues, certainly those that can be addressed by this type of finite-state model, do not appear to be the cause of this modelling inadequacy.

Discussion

Arguably, helicopter studies in the literature have tended to focus on main rotor modelling, and the mid- to high-speed range of the flight envelope. The novel features of this Paper are that the contemporary approach to rotor modelling in flight mechanics is applied equally to the tail rotor, and the helicopter's *forte* of hover and low speed flight has been examined. This, coupled with the unique insights afforded by the method of constrained or inverse simulation, has allowed a significant and quantified assessment to be made of the important developments in helicopter

mathematical modelling. For example, although the Peters' finite-state model used has undergone extensive validation, Ref. 18, its behaviour in simulation of role-related, large-amplitude flying has not been investigated. In addition exactly the same rotor model is used for both main and tail rotors. The fact that good comparisons are obtained with flight for main rotor collective, and relatively poor comparison for tail rotor collective, points to tail rotor-specific unmodelled effects. Main rotor wake and airframe aerodynamic interaction effects are the most probable cause of this, and the finite-state wake model does not provide the information for the simulation to address this. Chen's review paper, Ref. 6, indicated that computing improvements may one day allow non finite-state wake models to be used in flight simulation applications. Peter's finite-state model is still however *de rigeur* in these applications, but it is argued that the evidence in this Paper suggests that effort ought to go into non finite-state models.

One aspect of this approach to constrained or inverse simulation has been of special consideration in the work of Hess et al, Ref. 19 and that is the interval T .In addition Lin, Ref. 20 has postulated that this control strategy may be unstable for some values of T. This issue requires further special consideration for helicopter models capable of high bandwidth. It needs to be sufficiently short to capture observed features in the flight data - too short however, and the controls may be applied at an interval inconsistent with the mechanism by which rotor systems generate moments. The evidence in this Paper together with that in Ref. 12 is that the method is fairly robust, as the control application interval here is about two revolutions of the main rotor, whereas in Ref. 12 it is only one-half.

Conclusions

Constrained or inverse simulation of large-amplitude manoeuvres is possible with sophisticated helicopter mathematical models that employ an individual blade/blade element representation of both main and tail rotors. The rudimentary

step control strategy can give excellent attitude following, while retaining the capability of modelling the features of the control time histories measured in flight. Rigorous and consistent validation of the model at the limits of real aircraft performance has been possible, which has highlighted specific limitations in the simulation model.

These limitations are focused on the wake and induced velocity modelling. The contemporary finite-state induced velocity model is physically and numerically limited during flight into the vortex ring region. The limitation is quantified and affects the tail rotor model acutely. Further, the main rotor pitch and roll control required to fly the manoeuvres was shown to be insensitive to the harmonic components of induced velocity. Finally, the relatively poor prediction of tail rotor control required is attributed to unmodelled aerodynamic interactions. This latter issue can only be addressed by non finite-state wake models such as those of prescribed- or free-wake form.

References

1) Padfield, G. D., "Theoretical Modelling for Helicopter Flight Dynamics: Development and Validation," *Proceedings of the International Congress of the Aeronautical Sciences*, Jerusalem, Israel, 1988.

2) Houston, S. S., "Rotorcraft Aeromechanics Simulation for Control Analysis - Mathematical Model Definition", University of Glasgow Dept. of Aerospace Engineering Internal Report No. 9123, 1991.

3) Lehmann, G., Oertel, C-H., Gelhaar, B., "A New Approach in Helicopter Real-Time Simulation," *Proceedings of the 15th. European Rotorcraft Forum*, Amsterdam, The Netherlands, 1989.

4) DuVal, R. W., "A Real-Time Blade-Element Helicopter Simulation for Handling Qualities Analysis," *Proceedings of the 15th. European Rotorcraft Forum*, Amsterdam, The Netherlands, 1989.

5) Meerwijk, L., Brouwer, W., "Real-Time Helicopter Simulation Using the Blade-Element Method," *Proceedings of the 17th. European Rotorcraft Forum*, Berlin, Germany. ISBN 3 922010 66 0, 1989.

6) Chen, R. T. N., "A Survey of Non-Uniform Inflow Models for Rotorcraft Flight Dynamics and Control Applications," *Proceedings of the 15th. European Rotorcraft Forum*, Amsterdam, The Netherlands, 1989.

7) Gaonkar, G. H., Peters, D. A., "A Review of Dynamic Inflow Modeling for Rotorcraft Flight Dynamics," *Vertica*, Vol. 12, No. 3, 1988, pp. 213-242.

8) Peters, D. A., HaQuang, N., "Dynamic Inflow for Practical Applications," *Journal of the American Helicopter Society*, Vol. 33, No. 4, 1988.

9) Various, "Rotorcraft System Identification," AGARD Lecture Series 178, 1991.

10) Houston, S. S., "Validation of a Non-linear Individual Blade Rotorcraft Flight Dynamics Model Using a Perturbation Method,"*The Aeronautical Journal*, Vol. 98 No. 977, 1994, pp. 260-266.

11) Bradley, R., Padfield, G. D., Murray-Smith, D. J., Thomson, D. G., "Validation of Helicopter Mathematical Models," *Transactions of the Institute of Measurement and Control*, Vol. 12, No. 4, 1990.

12) Rutherford, S., Thomson, D. G., "Helicopter Inverse Simulation Incorporating an Individual Blade Rotor Model," *Proceedings of the 20th. International Congress of the Aeronautical Sciences*, Sorrento, Italy, 1996.

13) Tischler, M. B., "Digital Control of Highly Augmented Combat Rotorcraft," NASA TM-88346, 1987.

14) Turnour, S. R., Celi, R., "Modeling of Flexible Rotor Blades for Helicopter Flight Dynamics Applications," *Journal of the american Helicopter Society*, Vol. 41, No. 1, 1996, pp. 52-66.

15) Thomson, D. G., Bradley, R., "Development and Verification of an Algorithm for Helicopter Inverse Simulation," *Vertica*, Vol. 14, No. 2, 1990, pp.

16) Rutherford, S., Thomson, D. G., "Improved Methodology for Inverse Simulation," *The Aeronautical Journal*, Vol. 100, No. 993, 1996, pp.

17) Gao, C., Hess, R. A., "Inverse Simulation of Large-Amplitude Aircraft Manoeuvres," *Journal of Guidance, Control and Dynamics*, Vol. 16, No. 4, 1993, pp. 733-737.

18) Ellenreider, T. J., "Investigation of theDynamic Wake of a Model Rotor", Ph. D. Dissertation, University of Bristol, 1996.

19) Hess, R. A., Gao, C., Wang, S. H., "Generalized Technique for Inverse Simulation Applied to Aircraft Manoeuvres,", *Journal of Guidance*, Vol. 14, No. 5, 1991, pp. 920-926.

20) Lin, K-C., "Comment on Generalized Technique for Inverse Simulation Applied to Aircraft Manoeuvres," *Journal of Guidance*, Vol. 16, No. 6, 1993, pp. 1196-1197.

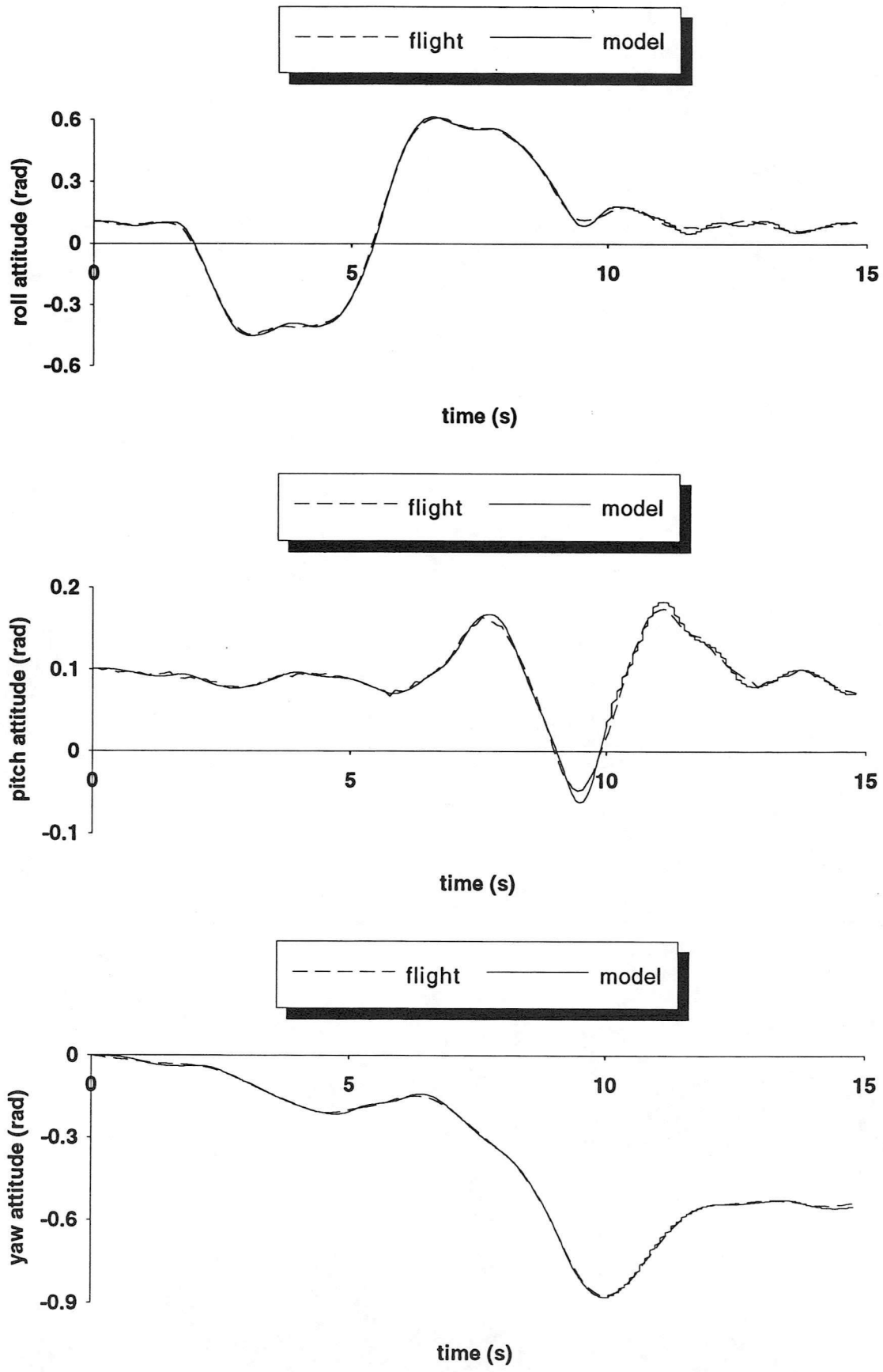

Figure 1a Comparison of flight and model aircraft attitude during left sidestep

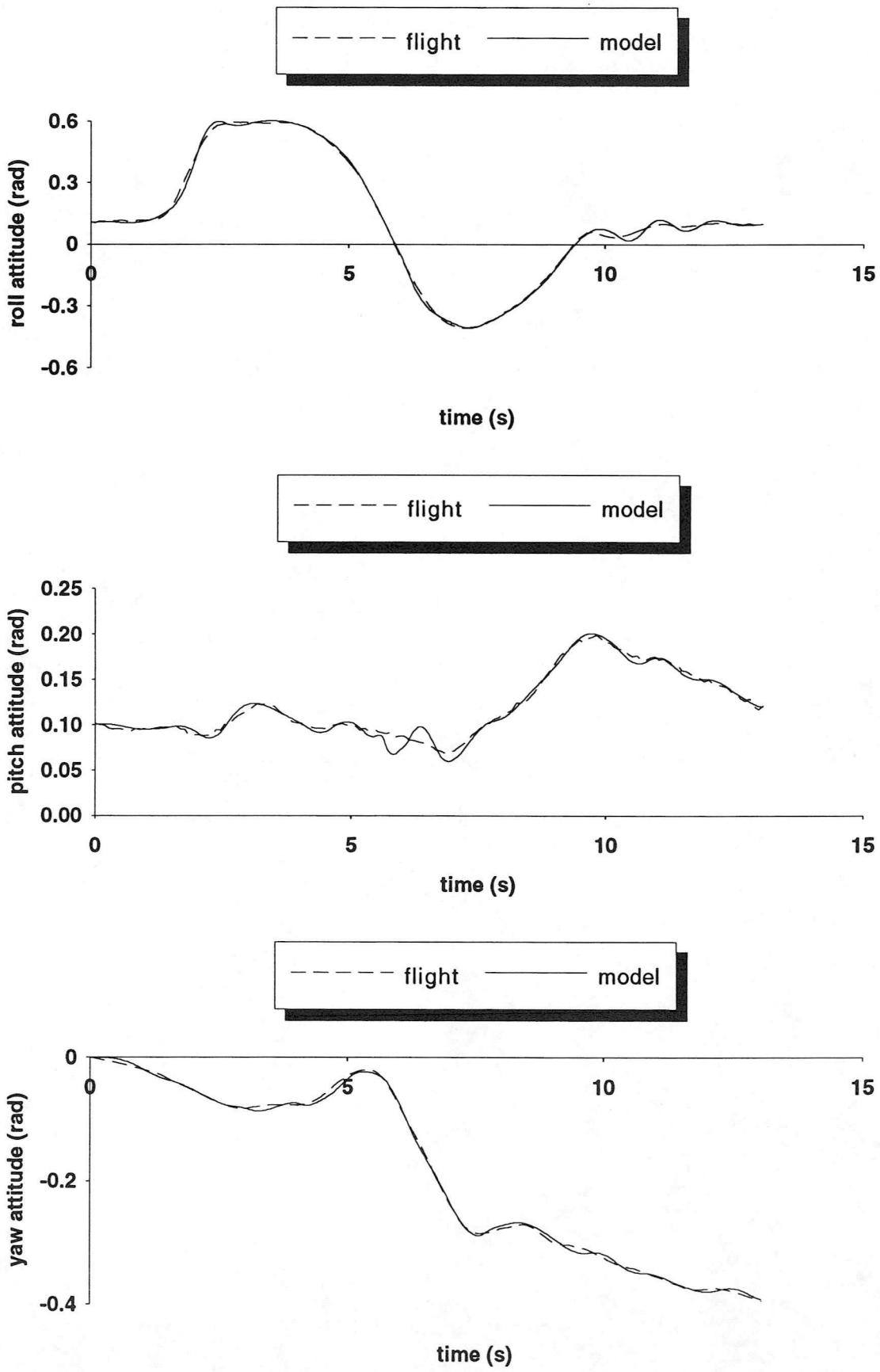

Figure 1b Comparison of flight and model aircraft attitude during right sidestep

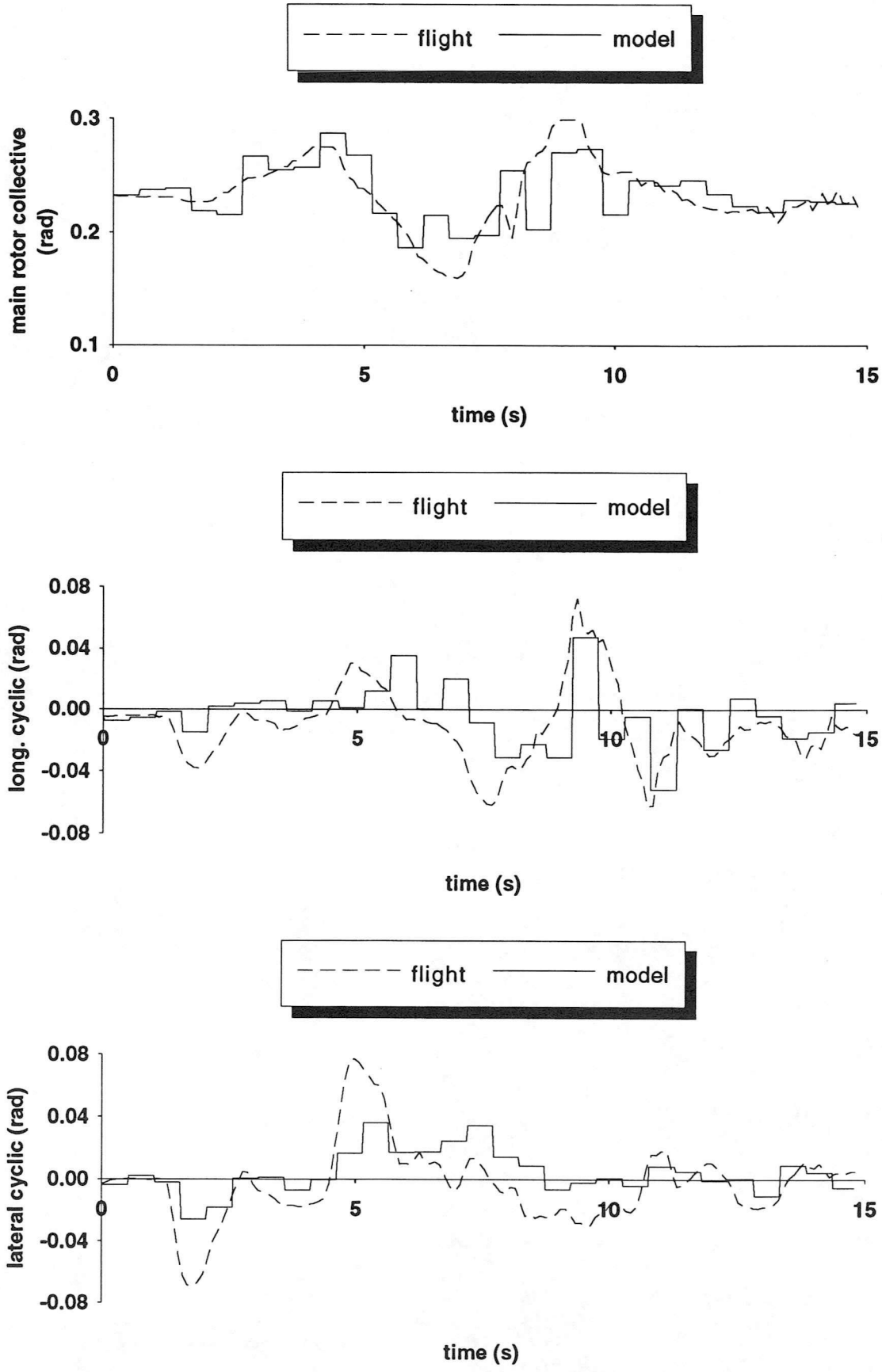

Figure 2a Comparsion of flight and model control angles during left sidestep

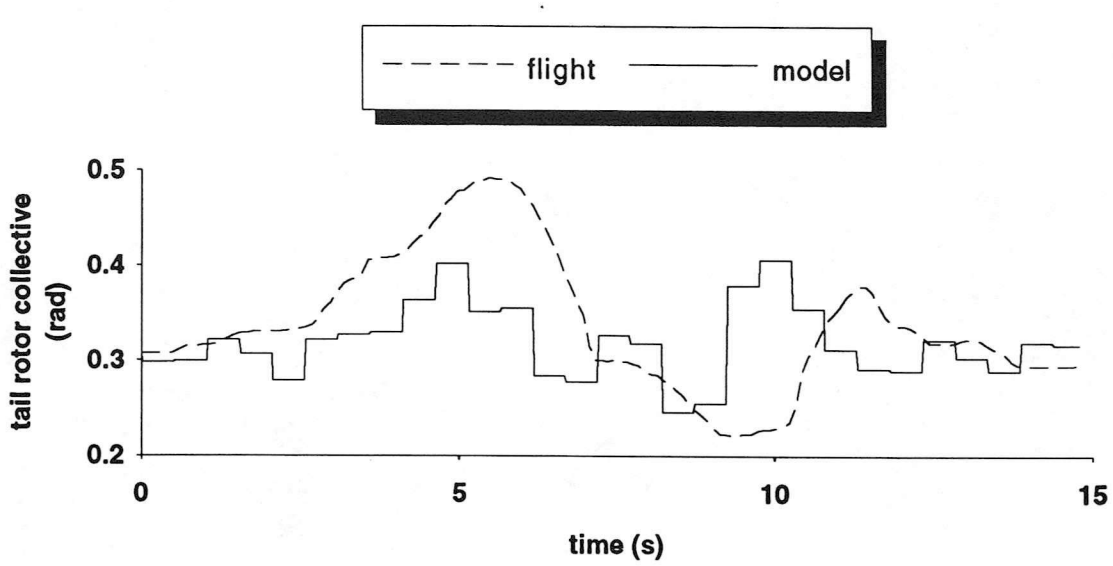

Figure 2a (concluded) Comparison of flight and model control angles during left sidestep

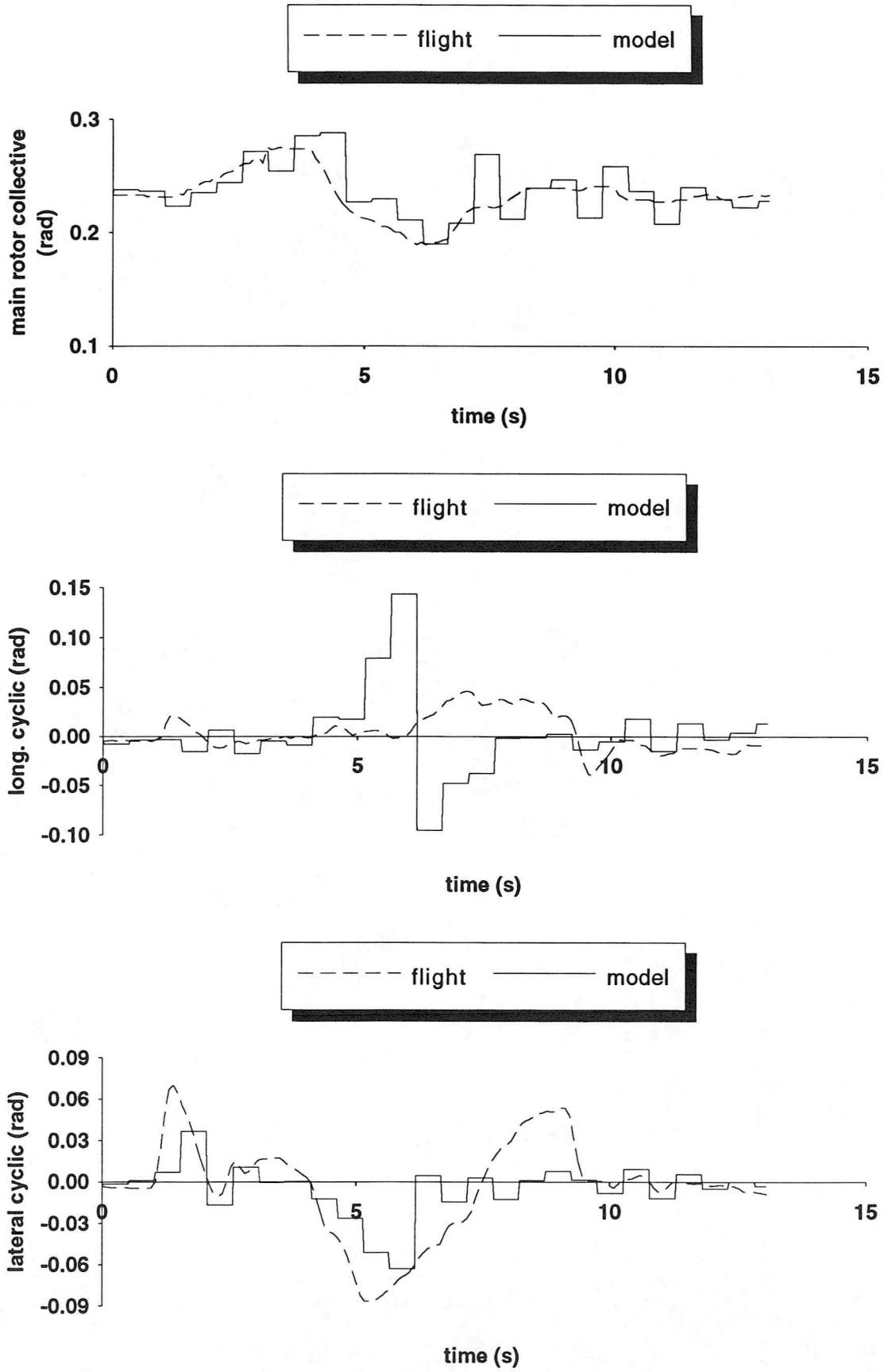

Figure 2b Comparison of flight and model control angles during right sidestep

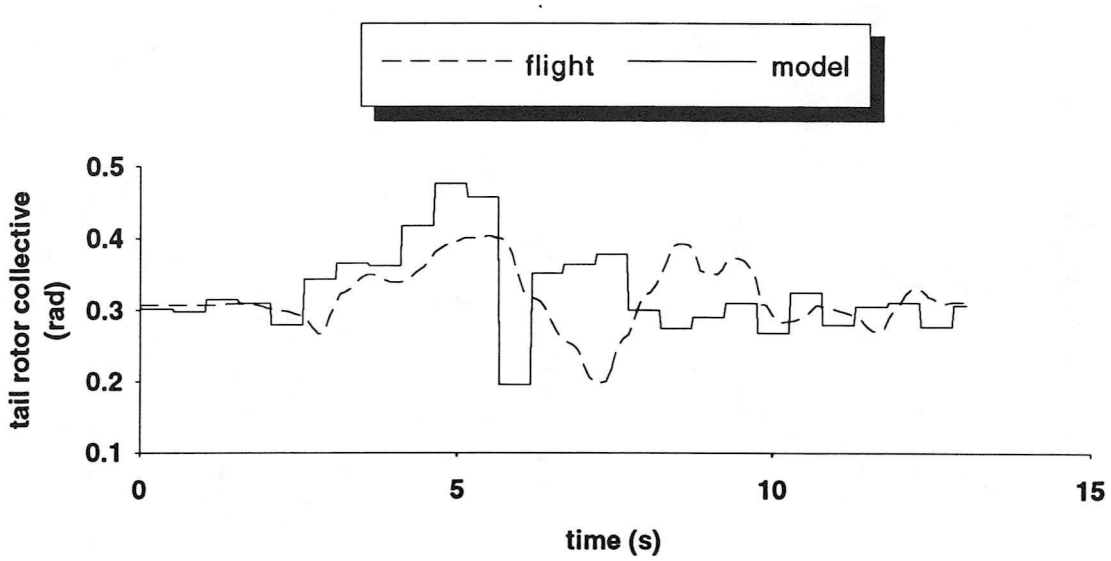

Figure 2b (concluded) Comparison of flight and model control angles during left sidestep

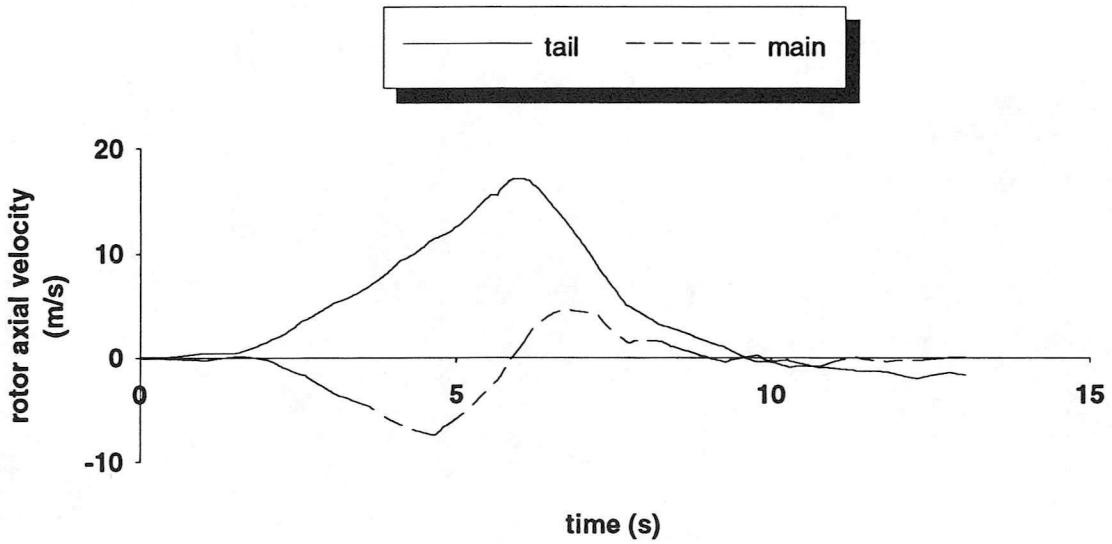

Figure 3 Model calculation of main and tail rotor axial velocity during right sidestep

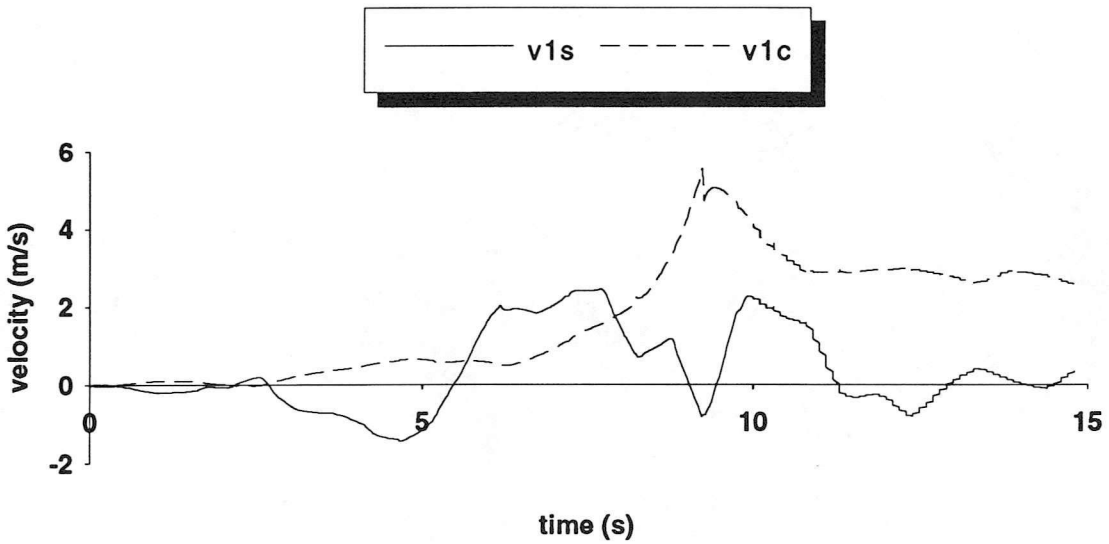

Figure 4 Tail rotor model harmonic induced velocity components during left sidestep

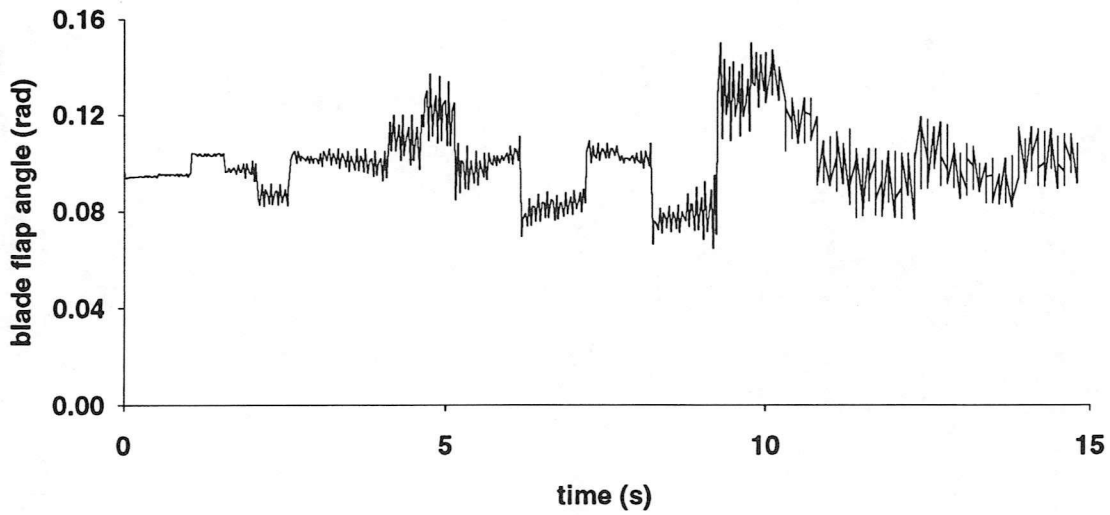

Figure 5 Tail rotor model blade flap during left sidestep

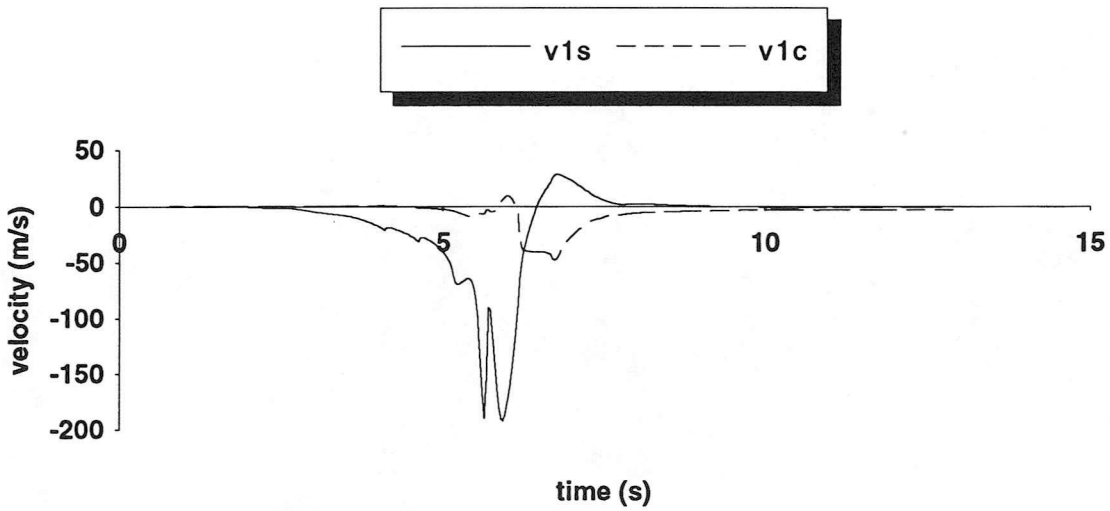

Figure 6 Tail rotor model harmonic induced velocity components during right sidestep

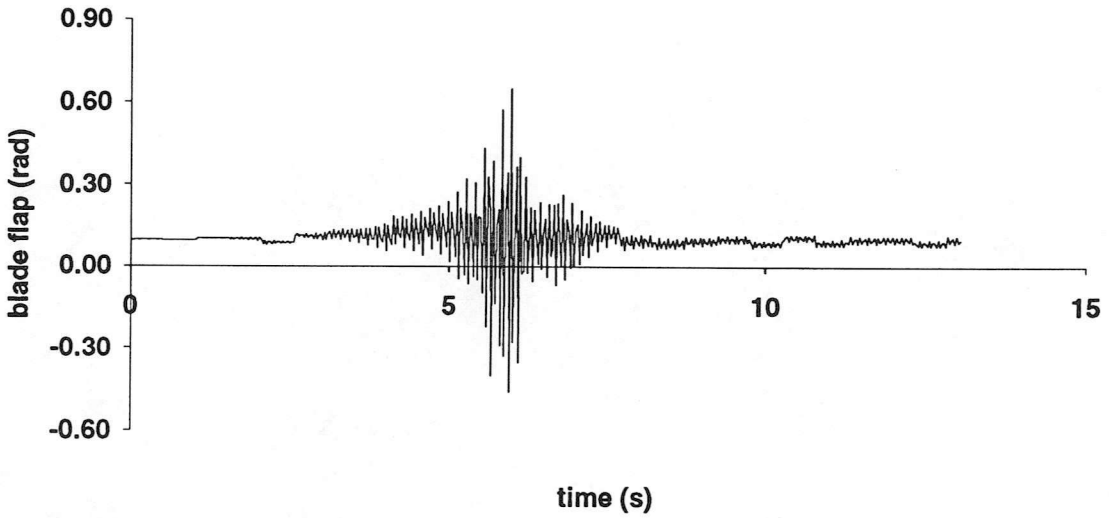

Figure 7 Tail rotor model blade flap during right sidestep

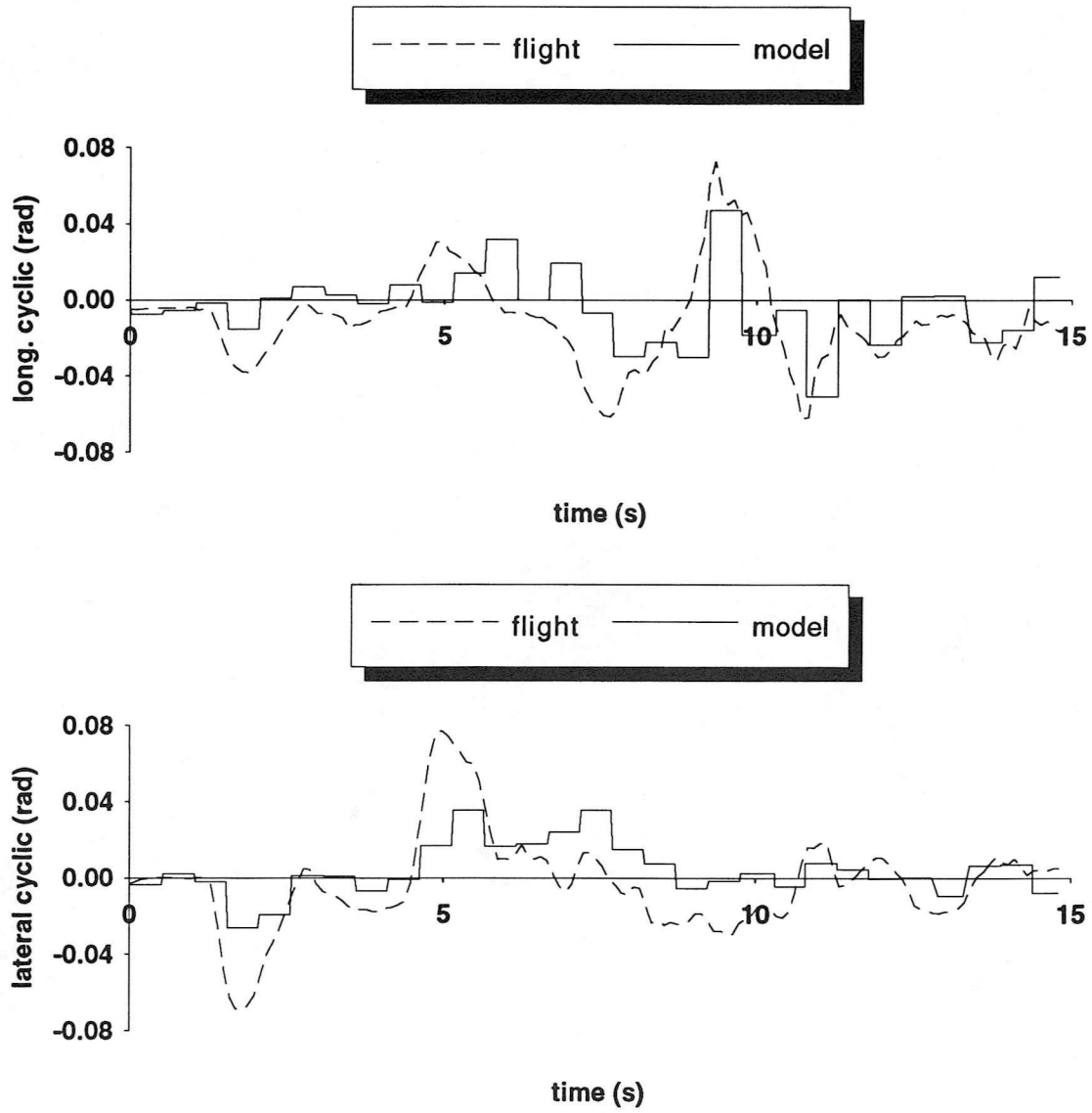

Figure 8 Comparison of flight and model cyclic pitch calculated with rigid-wake assumption

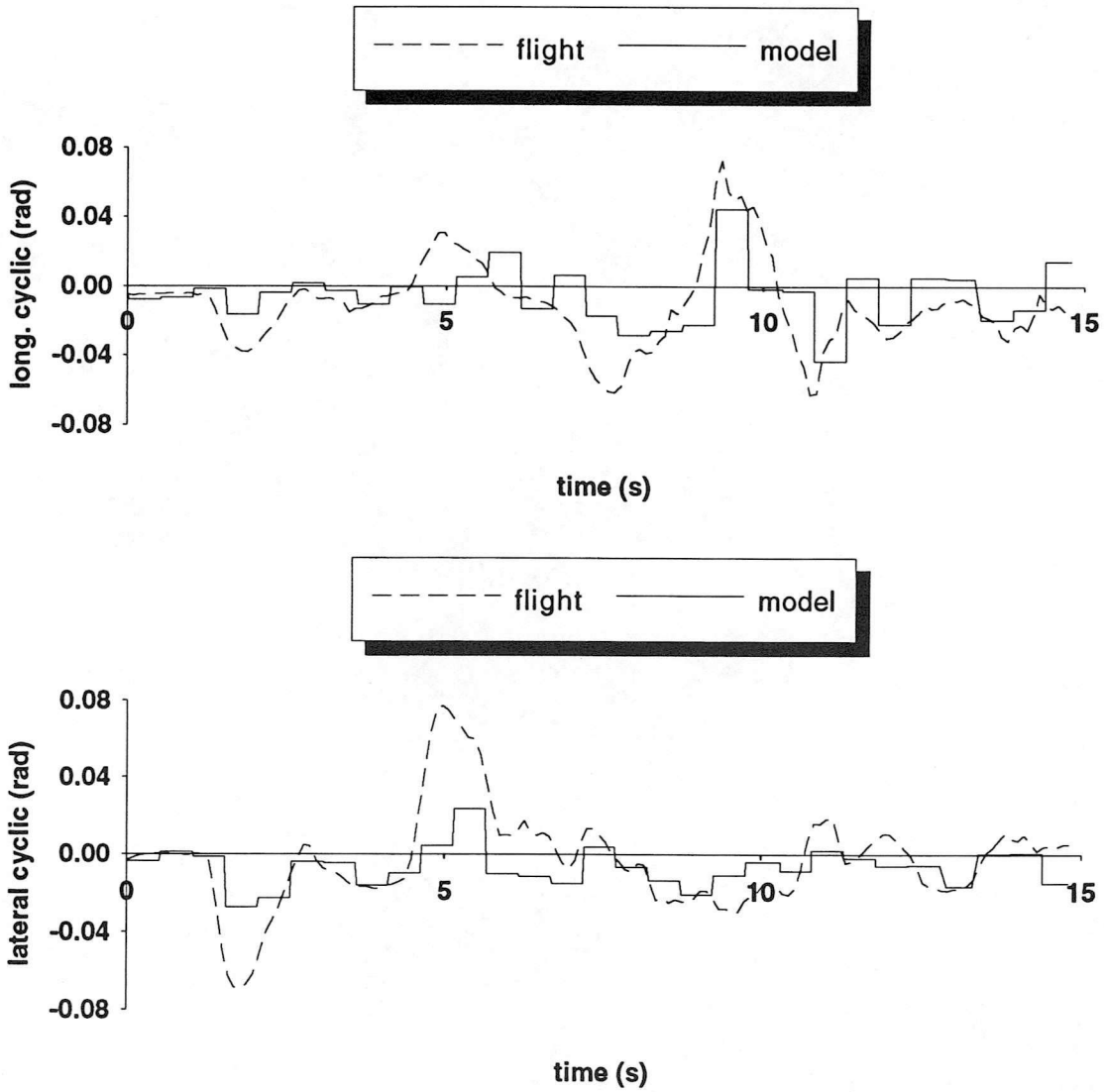

Figure 9 Comparison of flight and model cyclic pitch calculated with no harmonic components